CONTROLLED RELEASE OF RETINOL FROM BIOGLASS AND BIOCHAR PARTICLES – A THERMOGRAVIMETRIC ANALYSIS

Ioana-Lavinia LIXANDRU MATEI[1,2], Andreea Iuliana IONESCU[1], Andra-Ioana STĂNICĂ[3], Casen PANAITESCU[4], Gabriel VASILIEVICI[5], Dorin BOMBOȘ[4*], Bogdan Alexandru SAVA[2,6]

To limit excessive skin absorption of retinol, which may pose health risks, cosmetic creams can include adsorbents with specific textural properties. This study evaluates the influence of two such adsorbents, a bioglass and a biochar derived from grape seeds on retinol release. Their textural, crystalline, and surface characteristics were analyzed by N_2 adsorption/desorption, XRD, and SEM. Retinol release was assessed by TGA at various heating rates. Results showed that adsorbents with similar particle sizes but different pore distributions affect retinol desorption, with average pore diameter playing a key role.

Keywords: biochar, retinol, adsorbents, vitamin A, thermogravimetric analysis

1. Introduction

Retinol is necessary for the achievement of many functions of the human body, such as immune function, improvement of vision, cell development, but also for the maintenance of the skin and mucous membranes. As an ingredient in skin care products, retinol is used to reduce wrinkles and for other positive effects on skin aging [1]. Still the use of high doses of retinol can cause dry skin and hypervitaminosis so cosmetic products based on retinol should limit its rapid absorption into the body. This study aims to evaluate the influence of textural characteristics of some cosmetic adsorbents, such as bioglass and activated

[1] Pharm., Botanical SRL., Tatarani, Prahova County, Romania, e-mail: ioana@imarskin.com, hello@imarskin.com
[2] Prof., National University of Science and Technology POLITEHNICA Bucharest, Romania, e-mail: bogdan.sava2901@upb.ro
[3] Prof., "Toma Socolescu" Technological High school, Ploiesti, Romania, e-mail: ioanaandraa24@gmail.com
[4] Prof., Faculty of Petroleum Refining and Petrochemistry, Petroleum-Gas University of Ploiesti, Romania, e-mail: bombos.dorin@gmail.com, cpanaitescu@upg-ploiesti.ro
[5] Prof., National Institute for Research Development for Chemistry and Petrochemistry-ICECHIM-București, Bucharest, Romania, e-mail: gabi.vasilievici@gmail.com
[6] Prof., National Institute of Laser, Plasma and Radiation Physics – INFLPR, Magurele, Ilfov County, Romania

biochar, on the controlled release characteristics of retinol. Thus, an important aspect emerges the need to extend and influence the dosing period of vitamin A and improve its efficiency.

Active materials based on natural compounds are mentioned in specialized literature as a viable alternative to maintain the effectiveness of vitamin A. Active agents such as essential oils, natural compounds with antioxidants, antimicrobial and antiviral activity, is typically incorporated into various 1-5 powdery solids. [2,3,4,5,6,7,8,9,10,11,12,13,14,15,16,17,18,19]

In this study, we investigated for the first time the rate and behavior of vitamin A (retinol) release from bioactive glass powder and activated biochar impregnated at various concentrations using thermogravimetric analysis (TGA), with the aim of minimizing the potential side effects associated with the excessive transdermal absorption of retinol in cosmetic applications. The two natural adsorbents, bioglass and biochar derived from grape seeds, were thoroughly characterized in terms of their textural properties (via N_2 adsorption/desorption isotherms), surface morphology (SEM), crystalline structure (XRD), and particle size distribution (DLS).

Activated biochar demonstrated a significantly higher specific surface area and total pore volume than bioglass, along with a uniform mesoporous structure that enhances retinol adsorption and facilitates its gradual release. In contrast, bioglass exhibited a predominantly macroporous texture and partial crystallinity, which limited its adsorption efficiency. TGA profiles indicated that the desorption behavior of retinol was strongly dependent on the average pore diameter and the applied heating rate. While activated biochar showed variable mass loss correlated with temperature and thermal treatment conditions, bioglass presented a more uniform and limited release profile.

These findings support the use of activated biochar as a promising and efficient delivery platform for the controlled release of retinol in cosmetic formulations, contributing to enhanced efficacy and reduced dermal toxicity of vitamin A-based products.

2. Materials and Methods

All reagents used in this study are derived from Aldrich–Sigma and are reagent grade. Bioactive glasses Vitryxx® Bioactive Glass from SCHOTT was conditioned by washing with methanol, dried in an oven with air recirculation, at a temperature of 160° C over a period of 4 hours and then calcinated at a temperature of 550° C for 6 hours. Grape seeds were dried in an air circulation oven at 160° C for 8 hours and then ground in a ball mill. After grinding they were conditioned by the extraction of triglycerides and activation in the presence of water vapour. The extraction of triglycerides was performed with hexane at

reflux temperature of 69°C, the duration of the extraction process being 60 minutes and the activation was done in semi-continuous system, in the fixed adsorber reactor, in the presence of water vapors at a temperature of 650 °C for 6 hours.

The two adsorbents were characterized by the determination of textural characteristics, the determination of particle size distribution, of surface structure by scanning electron microscopy (SEM), and of crystallization behaviour by X-ray diffraction (XRD).

The determination of the textural characteristics of the two adsorbents was made using a gas sorption analyzer type NOVA 2200e (Quantachrome). Nitrogen adsorption/desorption isotherm was recorded at 77.35 K in a relative pressure range p/p0 between 0.005 and 1.0. The processing of the obtained data was carried out using a NovaWin software version 11.03. The specific surface area was determined from the standard BET equation (Brunauer-Emmett-Teller) and the total pore volume was estimated based on desorbed volume at a relative p/p0 pressure close to the unit, by the Barrett-Joyner-Halenda (BJH) method. The distribution of the pore size and the mesopore volume were obtained from the desorption branch of the isotherm by applying the BJH model. Before the adsorption measurements were made, the samples were degassed at 160°C in vacuum for 4 hours.

The particle size and particle size distribution of adsorbents were measured with a Nano ZS (Red badge) system using the DLS - Dynamic Light Scattering method. The method correlates the particle size by measuring their Brownian motion. Thus the relationship between the size of a particle and its speed generated by Brownian motion is given by the Stokes-Einstein equation. In order to determine the particle size distribution of the two adsorbents, the dispersion of the biochar particles was carried out in ethanol and the dispersion of the bioglass particles in water, and the stabilization of these suspensions was achieved by applying ultrasound over a period of 3 minutes. Particle size distribution, mean particle size, and polydispersity (PdI) were determined. Polydispersity is an indicator of particle distribution; thus, for a particle distribution as uniform as possible, the value of this indicator must be as close to zero as possible.

The microstructural morphologies were analysed using a Scios 2 HIVAC Dual-Beam FIB-SEM ultra-high resolution scanning electron microscope (SEM). The crystallisation behavior of the adsorbents tested was determined using a Bruker X-ray diffractometer equipped with a source having the following characteristics: Cu - Kα at 40 kV and 5 mA, 2θ range 1–40 at a rate 10°C min−1.

The deposition of retinol on the two powder adsorbents was carried out by impregnation using the pore-filling method, at a concentration of 5%. The volume of the pores is determined by adsorption of acetone, then the retinol is dissolved in

a quantity of acetone corresponding to the volume of the pores for each of the two adsorbents. The solution of retinol in acetone is dosed onto each of the pulverulent adsorbents with shaking and the solvent, acetone, is then removed by treating the adsorbent suspension in a circulating air oven at a temperature of 30 °C, until the weight is constant.

The evaluation of the controlled release rate of retinol adsorbed on the two types of adsorbents was carried out by its thermodesorption at different heating rates, ranging from 1 °C / min. and 10 °/min. The thermogravimetric (TGA) analyses of the two adsorbents impregnated with retinol were carried out on a TGA/-IST (Thermal Analysis System TGA 2, METTLER TOLEDO, Greifensee, Switzerland) in a nitrogen atmosphere and in the temperature range 25–700 °C.

3. Results and discussions

The liquid nitrogen adsorption isotherm on the active biochar practically overlaps with the desorption, indicating that the conditioning process of the active biochar precursor, lipid removal and steam activation favored the complete formation of pores (see Fig. 1). Also, the adsorption capacity of liquid nitrogen on active biochar has high values even at low pressure values.

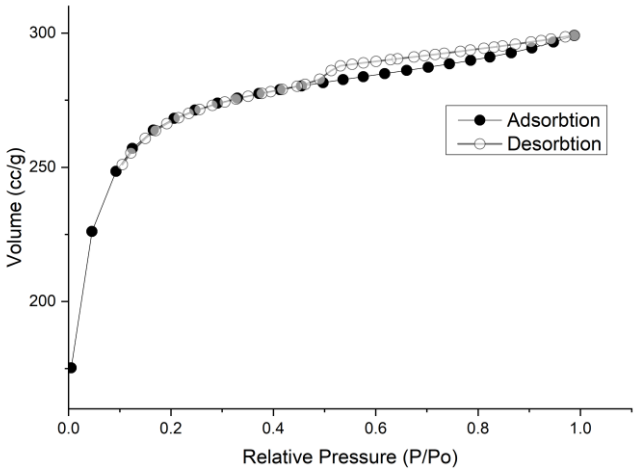

Fig. 1. N2 adsorption-desorption isotherms of activated biochar

The adsorption-desorption isotherm of liquid nitrogen on bioglass shows a much lower adsorption capacity of bioglass than that of the active biochar. Also, the higher volume of desorbed gas than adsorbed gas for relative pressure values higher than 0.2 is probably due to a more efficient desorption favored by weaker interactions between non-polar nitrogen molecule and the adsorbent molecules with higher polarity, as well as the release of gaseous products resulting from the calcination of bioglass (see Fig. 2).

Analysis of the pore size distribution curve of the activated biochar shows that the sample shows a relatively uniform distribution of pores with a high mesoporous content. The mesoporous structure favors the acceleration of surface processes, which enhances the adsorption and gradual release of the active principles into the adsorbent pores (see Fig. 3).

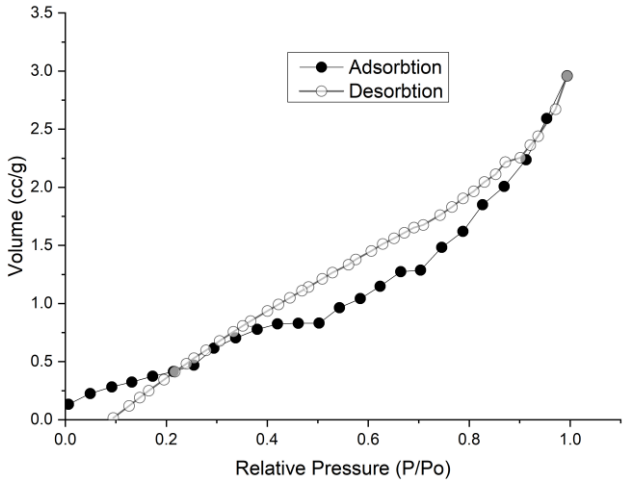

Fig. 2. N2 adsorption-desorption isotherms of bioglass

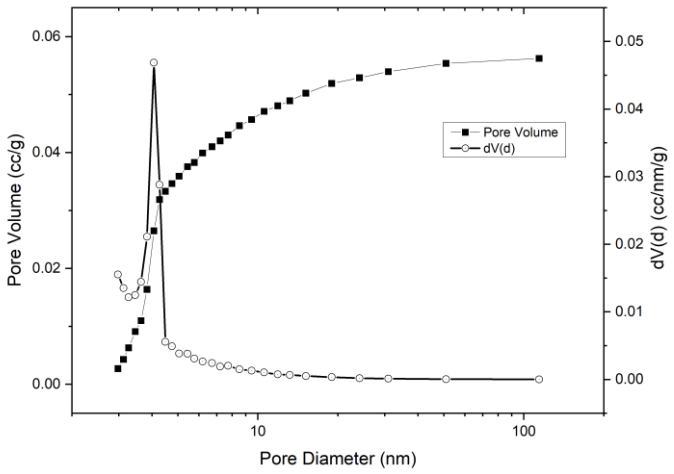

Fig. 3. The pore size distribution of activated biochar

The pore size distribution curve of a bioglass shows a broad pore size distribution with a high proportion of macropores and mesopores. The predominantly macroporous structure, with a maximum at pore diameter values greater than 3.3 nm, diminishes the adsorption capacity of the active principles in the adsorbent pores (see Fig. 4).

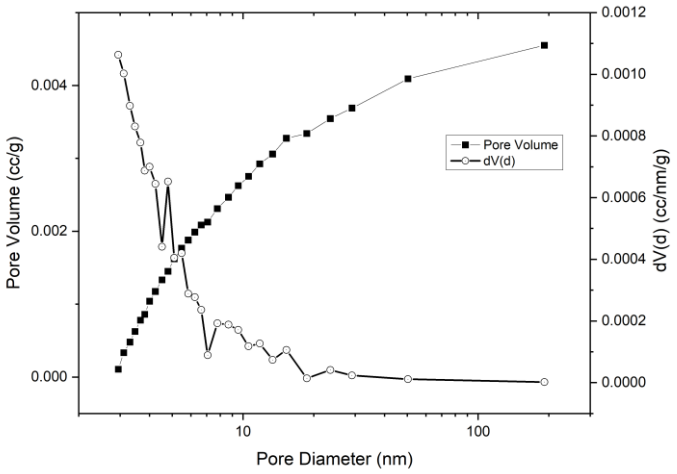

Fig. 4. The pore size distribution of the bioglass

The textural analyses determined the specific surface area, total pore volume and their average diameter (see Table 1). It is noted that the activated biochar shows much higher values of the specific surface area and of the total volume of pores compared to the bioglass.

Table 1

Textural characteristics of activated biochar and bioglass samples

Nr. Crt	Sample	Specific surface area (m2/g)	Total pore volume (cm3/g)	Mean pore diameter (nm)
1.	Activated biochar	106.818	0.107	3.294
2.	Bioglass	2.595	0.005	2.946

The particle size distribution of the two adsorbents, determined with the Zetasizer Nano device, is different as seen in Figs. 5 and 6. Thus, the distribution of the particle size of the biochar is binodal with maximums/ maxima situated at relatively close values while the particle size distribution of the bioglass is mononodal. The values of the sample sizes analyzed are close, the biochar sample presenting a range of variation relatively wider than that of the bioglass.

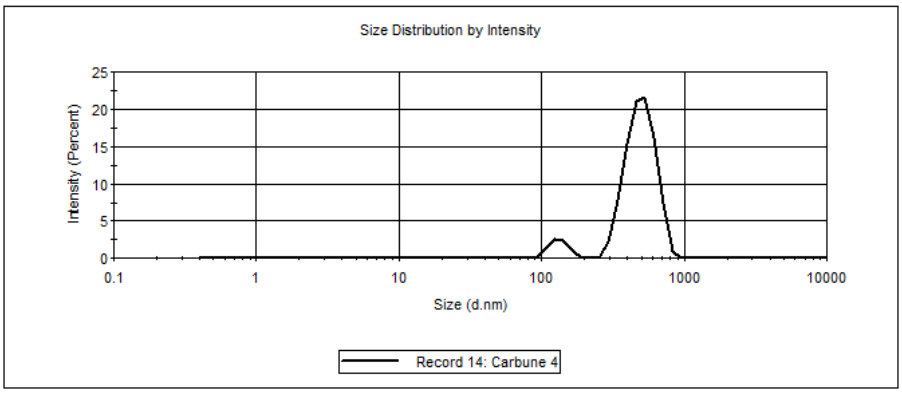

Fig. 5. Distribution of the size of the biochar particles

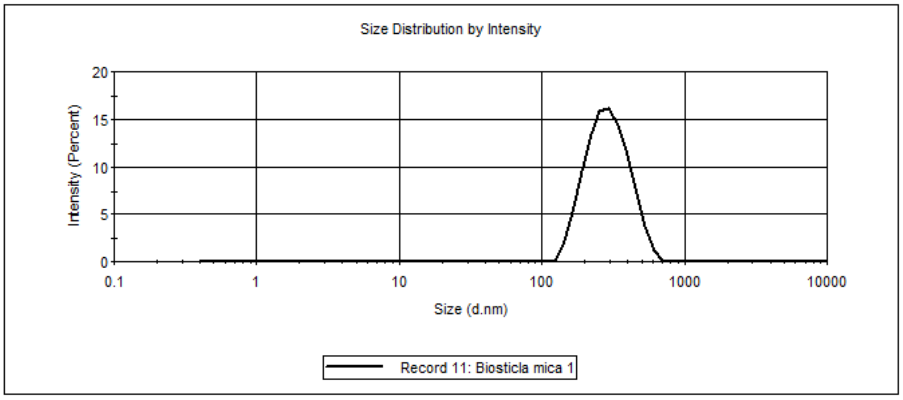

Fig. 6. Size distribution of the bioglass particles

The results of the measurements are presented in Table 2. The average particle size was over 70% higher in biochar than in bioglass and the polydispersity of the two samples indicates a close uniformity for the samples analyzed.

Table 2

Evaluation of particle size

Sample	Dm (nm)	PdI	Peak (Intensity)	Observations
Activated biochar	698	0.587	$P_1 = 503$, P2= 132	Large and polydisperse sizes; result in low reproducibility; aggregates of variable sizes are present.
Bioglass	403	0.522	$P_1 = 302$	Large and polydisperse sizes; aggregates of variable sizes are present. Reproducible measurements.

The evaluation of the presence of some adsorbent crystallinity zones was made by XRD analysis. XRD analysis of the activated biochar sample indicates an amorphous structure of the sample, while XRD analysis of the Bioglass sample indicates that part of the sample is crystalline, showing a maximum diffraction at approx. 33° which could be attributed to the presence of apatite (Figs. 7 A, B). These findings are in accord with data presented in the literature [20].

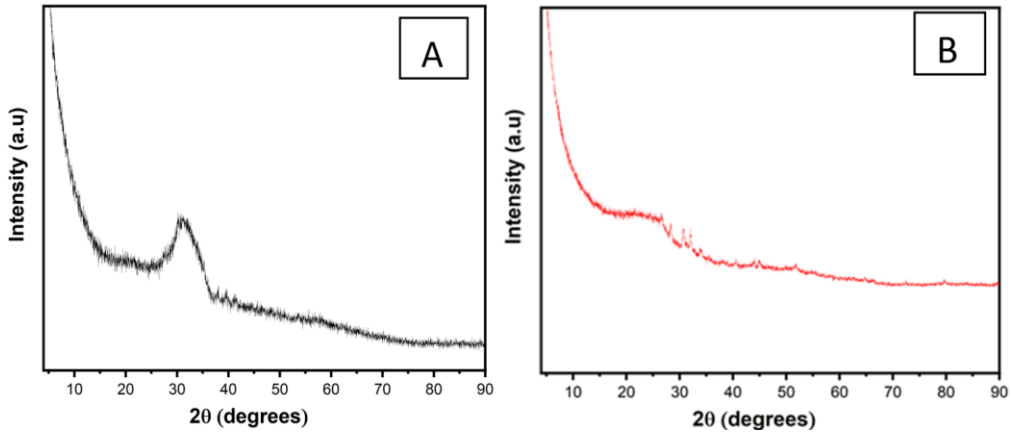

Fig. 7. XRD pattern for (A) activated biochar sample and (B) bioglass sample

The morphology of the cross-sections of the two adsorbents was determined by SEM analysis. From the images shown in Fig. 8, it is observed that the biochar sample shows an uneven distribution of surfaces that favor the formation of pores with different shapes and sizes.

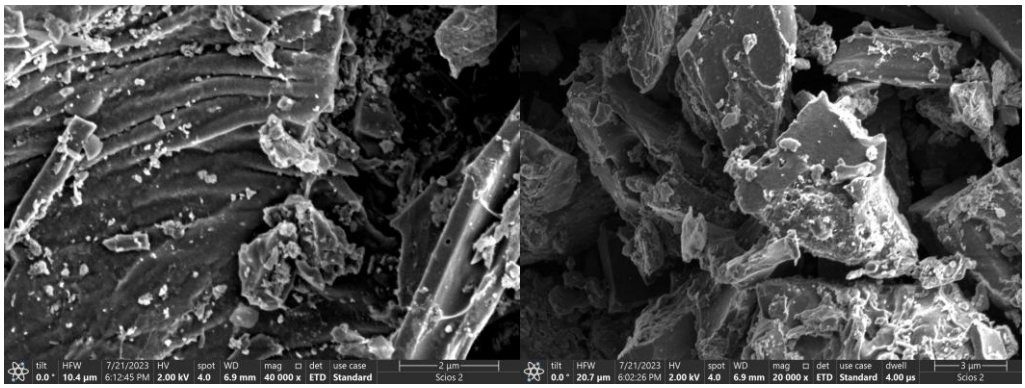

Fig. 8. Surface morphology for activated biochar sample

The calcined bioglass sample has relatively uniform surfaces, expected for a glassy material, as seen in the images shown in Fig. 9. These relatively large structures favor the predominant formation of macropores.

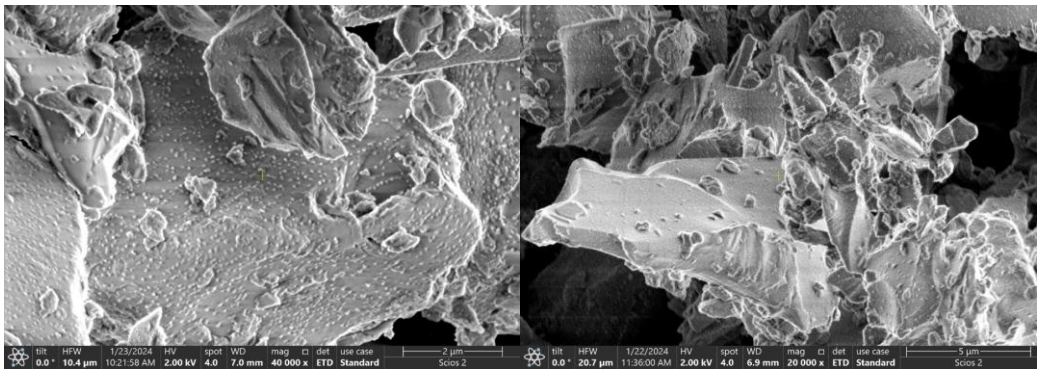

Fig. 9. Surface morphology for bioglass

The evaluation of the controlled release rate of the retinol adsorbed on the two types of adsorbents by its thermodesorption was performed at different heating speeds, ranging from 1 °C / min. and 10 °C /min. The thermogravimetric (TGA) analyses of the two retiol impregnated adsorbents are shown in Fig. 10 (A, B).

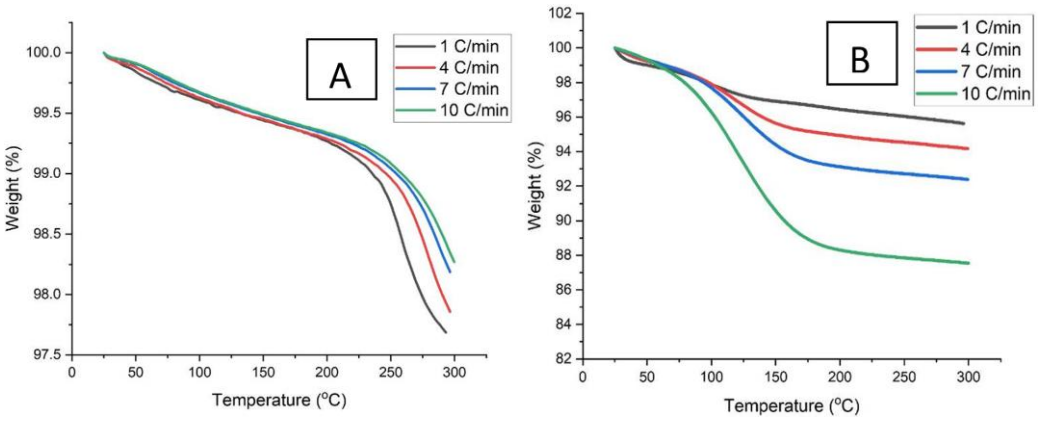

Fig. 10. TGA profile of (A) the activated biochar sample at different heating rates and (B) of the bioglass sample at different heating rates

According to the TG profile, there is a differentiated variation of mass loss of the biochar sample depending on the heating speed; thus, in the range of 50 - 300°C, both the slope of variation of the curves and the final value of the mass loss have different values. It is noted that at a low heating speed (1 °C /min.) the decrease in sample mass with the increase in temperature is much lower than in

the case of a higher heating speed (4 °C /min., 7 °C /min and 10 °C /min, respectively,) probably due to a wide distribution of pore size (Fig. 10A). In the case of the bioglass adsorbent, although the average particle size was about 70% smaller than that of the biochar particles, a smaller difference in mass loss was observed as a function of heating rate, for the same temperature range, both the slope of variation of the curves and the final value of the mass loss have much lower values than in the case of biochar. Thus, the mass loss of the samples with increasing temperature is very similar for temperatures up to 200 °C, and for temperatures above 200 °C the differences in mass loss are slightly higher but much lower than for biochar. In contrast to biochar, mass losses are higher at lower heating rates. This behaviour is probably due to a much lower total pore volume than in the case of biochar and a larger average bioglass pore size (Fig. 10B).

4. Conclusions

The biochar used for retinol adsorption was obtained by conditioning the grape seeds by extracting triglycerides/ lipides and activating them in the presence of water vapour. The liquid nitrogen adsorption isotherm obtained from the textural analysis revealed that after the removal of lipids from grape seeds, the pore formation is complete. Also, the pore size distribution curve of the activated biochar revealed a relatively uniform distribution of pores with a high mesopory content. The textural analysis of the bioglass used revealed a predominantly macroporous structure, which diminishes the adsorption capacity of the active principles in the adsorbent pores. XRD analysis of the activated biochar sample indicates an amorphous structure of the sample, while XRD analysis of the bioglass sample indicates that part of the sample is crystalline. As evidenced by the SEM analysis, the biochar sample shows an uneven distribution of the surfaces that favor the formation of pores with different shapes and sizes while the bioglass sample has relatively uniform surfaces, due to glassy structure.

R E F E R E N C E S

[1]. https://en.wikipedia.org/wiki/Retinol

[2]. *D. Liang, B. Feng, N. Li, L. Su, Z. Wang, F. Kong, Y. Bi,* "Preparation, characterization, and biological activity of Cinnamomum cassia essential oil nano-emulsion", Ultrasonics Sonochemistry, **Vol. 86**, May 2022, 106009

[3]. *AC. Guimarães, LM. Meireles, MF. Lemos, MCC. Guimarães, DC. Endringer, M. Fronza, R. Scherer*, "Antibacterial Activity of Terpenes and Terpenoids Present in Essential Oils", Molecules **Vol. 24**, no. 13, 2019, 2471

[4]. *A. Mihranyan, N. Ferraz, M. Strømme*, "Current status and future prospects of nanotechnology in cosmetics", Progress in Materials Science, **Vol. 57**, no. 5, June 2012, pp. 875-910.

[5]. *F. Khodadadi, M. Nikzad, S. Hamedi*, "Lignin nanoparticles as a promising nanomaterial for encapsulation of Rose damascene essential oil: Physicochemical, structural, antimicrobial and in-vitro release properties", Colloids and Surfaces A: Physicochemical and Engineering Aspects, **Vol. 687**, no. 20 April 2024, pp. 133580.

[6]. *L. Núñez, M D. Aquino, J. Chirife*, "Antifungal properties of clove oil (Eugenia caryophylata) in sugar solution", Brazilian Journal of Microbilogy, **Vol. 32**, 2001, pp. 123-126.

[7]. *RM. Hajishirkiaee, H. Ehtesabi, H. Latifi*, "Peppermint essential oil and ZnO nanoparticles: A green and effective combination for a cooling bilayer patch with antibacterial activity", Journal of Environmental Chemical Engineering, **Vol. 12**, no 3, June 2024, pp. 112833

[8]. *S. Zhao, Y. Li, Q. Li, X. Xia, Q. Chen, H. Liu, B. Kong*, "Characterization, release profile, and antibacterial properties of oregano essential oil nanoemulsions stabilized by soy protein isolate/tea saponin nanoparticles", Food Hydrocolloids, **Vol. 151**, June 2024, pp. 109856

[9]. *S. Pourshahrestani, E. Zeimaran, NA. Kadri, N. Mutlu, A.R. Boccaccin*, "Polymeric Hydrogel Systems as Emerging Biomaterial Platforms to Enable Hemostasis and Wound Healing", Advanced Healthcare Materials, **Vol. 9**, no. 20, September 2020, pp. 2000905

[10]. *S. Yousefi, P. Rajaei, L. Nateghi, HR. Nodeh, L. Rashidi*, "Encapsulation of sesamol and retinol using alginate and chitosan-coated W/O/W multiple emulsions containing Tween 80 and Span 80", International Journal of Biological Macromolecules, **Vol. 242**, Part 2, July 2023, pp. 124766

[11]. *K. Schuhladen, JA. Roether, AR. Boccaccini*, "Bioactive glasses meet phytotherapeutics: The potential of natural herbal medicines to extend the functionality of bioactive glasses", Biomaterials, **Vol. 217**, October 2019, pp. 119288

[12]. *YJ. Hwang, C. Oh, SG. Oh*, "Controlled release of retinol from silica particles prepared in O/W/O emulsion: the effects of surfactants and polymers", Journal of Controlled Release, **Vol. 106**, no. 3, September 2005, pp. 339-349

[13]. *H. Saad, A. Ayed, M. Srasra, M, Mezni, R. Essid, S. Jallouli, O. Tabbene, E. Srasra*. "Smectite Clay Nanoparticles as a Sustained Release System for Cinnamom Essential Oil Targeting Candida albicans". Chemistry Africa **Vol. 7**, 2024, pp. 3185–3200

[14]. *N. Srinatha, S. Battu, BA. Vishwanath*, "Microsponges: a promising frontier for prolonged release-current perspectives and patents". Beni-Suef Univ J Basic Appl Sci, **Vol. 13**, no. 60, June 2024,

[15]. *S. Niknafs, MMY. Meijer, AA. Khaskheli, E. Roura*, "In ovo delivery of oregano essential oil activated xenobiotic detoxification and lipid metabolism at hatch in broiler chickens", Poultry Science, **Vol. 103**, February 2024, pp. 103321

[16]. *KG. Golezani, S. Rahimzadeh*, "The biochar-based nanocomposites influence the quantity, quality and antioxidant activity of essential oil in dill seeds under salt stress", Scientific Reports **vol. 12**, no. 21903, December 2022.

[17]. *Y. Xu, Z.Ji, B. Wei, S. Kong, Y. Wang, C. Li, H. Wang*, "Preparation and biological studies of Chinese propolis essential oil-loaded chitosan/hydroxyapatite biomimetic material", Food Measure, **Vol.18**, October 2023, pp. 382–392

[18]. *P. Taherian, MS. Nourbakhsh, AA. Mehrizi. M. Hashemi*, "Encapsulation of Frankincense Essential Oil by Microfluidic and Bulk Approaches: A Comparative Study". Fibers and Polym **Vol. 23**, September 2022, pp 2970–2980

[19]. *M. Wahdan, E. Tolba, A. Negm, FF. El-Senduny, OY*. Elkhawaga, "Potential of βC-Loaded Silica Nanoparticles in the Management of L-NAME –Induced Hypertension in Experimental Rats". BioNanoSci. **Vol. 12**, September 2022, pp. 1315–1328

[20]. *I.L. Lixandru Matei, BA Sava, C. Sarosi, C. Duşescu-Vasile, DR. Popovici, AI. Ionescu, D. Bombos, M. Băjan, R. Doukeh,* "The Influence of PEG 4000 on the Physical and Microstructural Properties of 58S Bioactive Glasses", Nanomaterials, **Vol. 14**, 2024, pp. 1323